Caging Dynamics in a Granular Fluid

P. M. Reis,* R. A. Ingale, and M. D. Shattuck†

Benjamin Levich Institute, The City College of the City University of New York, 140th Street and Convent Avenue, New York, New York 10031, USA

(Received 17 October 2006; published 30 April 2007)

We report an experimental investigation of the caging motion in a uniformly heated granular fluid for a wide range of filling fractions, ϕ. At low ϕ the classic diffusive behavior of a fluid is observed. However, as ϕ is increased, temporary cages develop and particles become increasingly trapped by their neighbors. We statistically analyze particle trajectories and observe a number of robust features typically associated with dense molecular liquids and colloids. Even though our monodisperse and quasi-2D system is known to not exhibit a glass transition, we still observe many of the precursors usually associated with glassy dynamics. We speculate that this is due to a process of structural arrest provided, in our case, by the presence of crystallization.

DOI: 10.1103/PhysRevLett.98.188301 PACS numbers: 47.57.Gc, 05.70.Ln, 61.20.Lc, 64.70.Dv

In additional to being of great industrial and geological importance, granular materials are of fundamental interest due to their strong nonequilibrium nature [1]. Ensembles of granular particles are intrinsically dissipative and any dynamical study must involve energy injection. These ingredients make the understanding of granular assemblies a challenging endeavor, and a general theoretical framework is still lacking. Some progress has been made in the fast dilute regime [2], treating the system as a nonequilibrium steady state in which energy injection balances dissipation, but the dense case remains an open question. One avenue of research has been to borrow concepts from other dense particulate systems such as colloids, suspensions, and emulsions, or even molecular glass formers [3], but *a priori*, it is not obvious that such analogies are valid due to the enormous differences in length scales and the mechanism of energy supply. However, one common feature in all of these seemingly disparate systems is the presence of *cages*: each particle is temporarily trapped by its neighbors and then moves in short bursts due to nearby cooperative motion. This results in highly heterogeneous motion and slowing down of the dynamics. In molecular systems, this behavior is typically observed indirectly from scattering experiments [4]. In colloids, however, caging motion has been observed directly through microscopy, in both 3D [5] and quasi-2D [6] geometries. A large number of theoretical [7,8] and numerical [9,10] studies have set out to further investigate the importance of this heterogeneous dynamics. The relevance of the *caging* in driven granular materials [11,12] and air-fluidized particle systems [13] has only recently started to be addressed. In particular, Dauchot *et al.* [12] have reported on a granular system driven by cyclic shear where they observed many ''glasslike'' features, but for a single value of the filling fraction.

In this Letter we present a novel dynamical study of a monodisperse, quasi-2D granular fluid [14], in which the particles are excited by a spacially uniform stocastic forcing. In our system, the filling fraction, ϕ, can be varied from a single particle to hexagonal close packing. We have shown that the structural configurations of this nonequilibrium steady state are the same as those of equilibrium hard disks [14]. In particular, the system does not have an amorphous dense phase but instead exhibits the following phase diagram: an isotropic fluid phase $\phi < \phi_l = 0.652$, a crystaline solid phase $\phi > \phi_s = 0.719$, and an intermediate phase $\phi_l < \phi < \phi_s$ consistent with a hexatic phase [15]. The phase boundaries, ϕ_l (*liquidus* point) and ϕ_s (*solidus point*), are determined by structure alone [14]. Here, we explore the dynamics of these phases through single particle trajectories, focusing on the caging dynamics seen in the intermediate phase. In Fig. 1 we present typical single particle trajectories for filling fractions in each of the three phases. Simple fluid behavior is observed at low ϕ, characterized by random diffusion [Fig. 1(a)]. Above crystallization ($\phi > \phi_s$) particles become fully arrested by their six hexagonally packed neighbors [Fig. 1(c)]. In the intermediate phase, we see a mixture of these behaviors [Fig. 1(b)]. At short times, particles are temporarily trapped in cages formed by their neighbors, but at long times they diffuse from cage to cage. We will use the mean square displacement (MSD) and the intermediate scattering function (ISF) to show that the caging

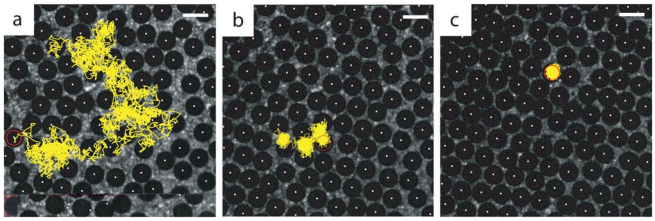

FIG. 1 (color online). Experimental frames with superposed typical trajectories of a single particle: (a) $\phi = 0.567$, (b) $\phi = 0.701$, and (c) $\phi = 0.749$. Note that even though only a single trajectory is shown for each ϕ, particle tracking and statistics were performed over all particles within the imaging window. The scale bar is 2 mm.

dynamics seen here is qualitatively identical to that of dense molecular and colloidal systems [4,5] and supercooled liquids [16]. This is surprising since our experiment is fundamentally different. The associated length scales of our granular system are typically 3–7 orders of magnitude larger than those of molecular systems and colloids. Moreover, the steady states we study are inherently far from equilibrium since energy is both injected (through vibration) and dissipated in interparticle inelastic collisions and frictional contacts.

Our experimental apparatus consists of vertically vibrated, $D = 1.19$ mm diameter stainless steel spheres confined between two $85.3D$ diameter horizontal glass plates, separated by $1.6D$, which constrain the particle motion to be quasi-2D. Our system is described in more detail in [14,17] and improves on Olafsen and Urbach's similar system [18] by using a roughened bottom plate. Particle collisions with the rough surface randomize the horizontal velocities better than a flat surface and allow us to study a wide range of filling fractions ($1.4 \times 10^{-4} < \phi < 0.8$) [17]. We sinusoidally vibrate the system with a frequency $f = 50$ Hz and a maximum acceleration equal to 4 times gravity, but the structure and dynamics of the system are independent of the forcing for a wide range of parameters [17]. To ensure repeatable initial conditions, we start with all particles hexagonally packed near the boundary. A steady state is reached by waiting for 12 000 vibration cycles before 10 seconds of data are acquired. We record the dynamics in a (12.62×12.62 mm^2) central region using a high-speed camera at 480 Hz and track the trajectories of all particles.

We first analyze the particle trajectories by measuring the mean square displacement defined as $M(t) = \langle [r(t) - r(0)]^2 \rangle$, where $r(t)$ is the position of a particle at time t, $r(0)$ is its initial position, the brackets $\langle . \rangle$ signify ensemble averaging over many realizations, and time invariance is assumed. The MSD for a range of ϕ are shown in Fig. 2. For the case of a single particle in the cell (curve marked with + in Fig. 2), the motion at short times is ballistic, and $M(t) \sim t^{\alpha}$, where $\alpha \sim 2$ ($\alpha = 2$ for pure ballistic motion). At later times, the particle moves diffusively and the slope of $M(t)$ tends to $\alpha = 1$. This shows that the trajectory of a single particle is indeed randomized across the cell. For all ϕ, the motion at early times is superdiffusive with $\alpha \sim 2$ showing ballistic motion. For $\phi < 0.719$ the motion always becomes diffusive at long times with $M(t) \sim t$. Eventually, this becomes increasingly noisy due to the lack of statistics in the time averaging. For $\phi > 0.719$ the particles are trapped by their six hexagonally packed neighbors, and $M(t)$ levels off to a constant value set by the lattice spacing. In the intermediate phase, however, a plateau emerges at intermediate times where the motion is subdiffusive with $0 < \alpha < 1$. This plateau appears slightly before the liquidus point but gradually becomes increasingly visible above ϕ_l (marked as $*$ in Fig. 2 to aid in locating the curves in the phase diagram). This represents

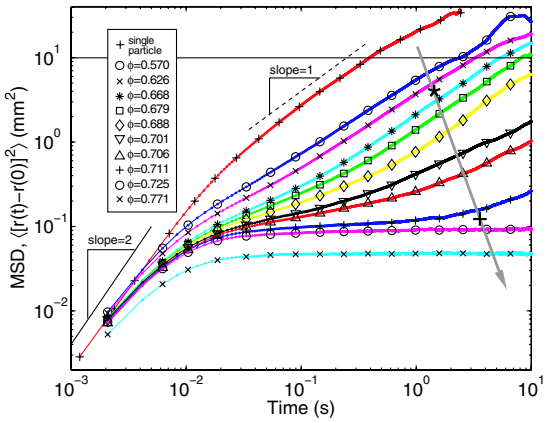

FIG. 2 (color online). Time dependence of the MSD for filling fractions shown in the box. The curve marked with + is for a single particle in the cell. The arrow points in the direction of increasing ϕ. Along the arrow, the symbols ($*$) and (+) are located at ϕ_l and ϕ_s, respectively, to aid locate the curves in the fluid's phase diagram. The horizontal line at 9.954 mm^2 corresponds to the square of 1/4th of the linear dimension of the imaging window, above which finite system size effects become important.

the slowing down due to the cage effect shown in Fig. 1(b). A similar dependence of $M(t)$ has recently been observed in a quasi-2D system of bidispersed particles fluidized by a uniform upflow of air [13].

Another classic measure in the study of dense liquid phases is the intermediate scattering function [4] which is defined as

$$F_s(\mathbf{q}, t) = \frac{1}{N} \sum_j \langle \exp(-i\mathbf{q} \cdot [\mathbf{r}_j(t) - \mathbf{r}_j(0)]) \rangle, \qquad (1)$$

where $\mathbf{q}$ is a wave number and $\mathbf{r}_j(t)$ is the trajectory of particle j out of N particles in the system. This measure is widely used in colloids since it is readily available through light scattering experiments [4] and is, essentially, a measure of the time decorrelation of the positional wave vectors. In dense colloids and supercooled liquids, $F_s(t, q)$ captures the relaxation due to caging in the form of a two-step relaxation: (1) the fast (early time) β relaxation which corresponds to the diffusion inside the cage followed by (2) the α relaxation corresponding to the time it takes for the particle to diffuse out of the cage.

In Fig. 3 we plot $F_s(t)$ for the wave vector $qD = 2.14$ ($q = 1.8$ mm^{-1}) for various values of ϕ. As expected, in the crystal phase ($\phi > 0.719$) F_s levels at a value close to 1 and little decorrelation occurs, since each particle is fully trapped. In the fluid phase, F_s rapidly decays as particles move across the cell diffusively and the initial positional wave vector quickly decorrelates. In the intermediate phase we observe the classic α and β two-step relaxation; there is a clear intermediate plateau and the α relaxation occurs at increasingly longer time scales, as ϕ is increased. As for

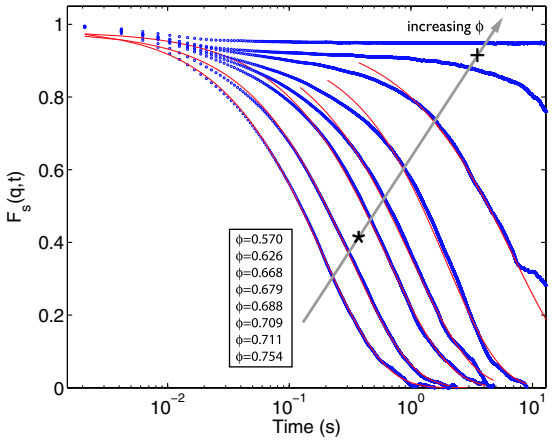

FIG. 3 (color online). Time dependence of the intermediate scattering function, with $qD = 2.14$, for various filling fractions (numerical values of ϕ given in the box). The arrow points in the direction of increasing ϕ. Along the arrow, the symbols $(*)$ and $(+)$ are located at ϕ_l and ϕ_s, respectively, to aid locate the curves in the fluid's phase diagram. The solid lines are fits to Eq. (2).

the MSD before, this two-step relaxation becomes particularly visible above the liquidus point, even though it can already be seen just before ϕ_l (marked as $*$ in Fig. 3 to help locate the curves in the phase diagram). For each value of ϕ, the α relaxation at late times is well described by a stretched exponential of the form

$$F_s(q, t) \sim \exp\{-[t/\tau(q)]^{\beta(q)}\}, \tag{2}$$

where $\tau(q)$ is a relaxation time and the stretching exponent is typically $\beta(q) \leq 1$. Fits of this stretched exponential form to the experimental data are shown as solid lines in Fig. 3. It is interesting to note that this behavior is in good agreement with the predictions of mode coupling theory (MCT) [7]. This is highly surprising since MCT has been developed for thermal fluids and is not known to apply to nonequilibrium systems such as ours.

We now focus on the q dependence of both the relaxation time $\tau(q)$ [Fig. 4(a)] and the exponent $\beta(q)$ [Fig. 4(b)], for various values of ϕ. We defined $\tau(q)$ as the time it takes for the experimental curves of F_s to fall to a level of $1/e$, i.e., $F_s(\tau) = 1/e$. The stretching exponent $\beta(q)$ is the local slope of the quantity $\log[-\log(F_s)]$ in the neighborhood of τ. At low filling fractions, the scaling with τ with q is consistent with $\tau \sim q^{-2}$. As the filling fraction is increased, this scaling continues to hold but only up to a cutoff value above which (length scale below which) it sharply drops. This cutoff length scale can be associated with a characteristic size of the cage, which becomes increasingly smaller as ϕ is increased. On the other hand, β, the local exponent, tends to one at small q but decreases progressively below one for higher filling fractions and F_s becomes increasingly stretched. These findings can now be combined and interpreted as follows. For

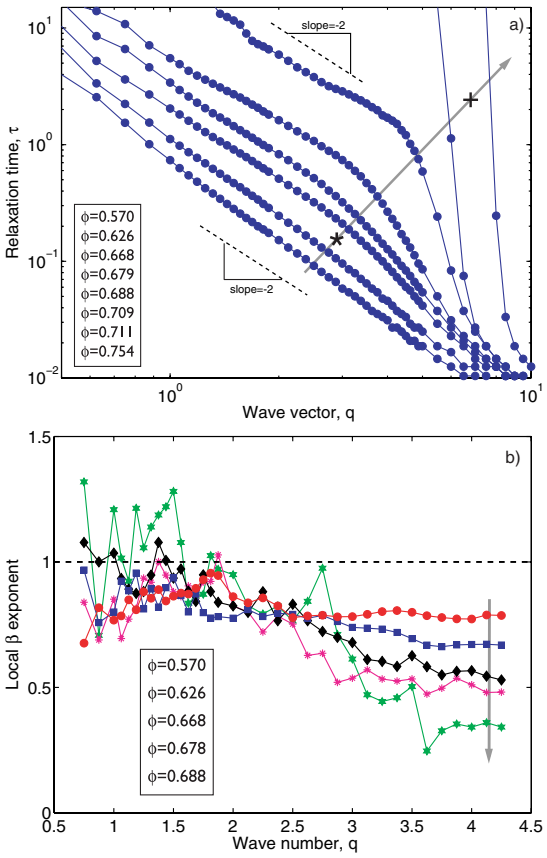

FIG. 4 (color online). (a) Wave vector dependence of the relaxation time, τ, and (b) local stretching exponent, β, for various values of filling fraction. The arrows point in the direction of increasing ϕ, and the numerical values of ϕ are given in the boxes. Along the arrow, the symbols $(*)$ and $(+)$ are located at ϕ_l and ϕ_s, respectively.

small q (i.e., large length scales), if $\tau \sim q^{-2}$ and $\beta(q) \to 1$, together they imply that $F_s(q, t) \sim \exp(-Dq^2 t)$. This is the result for classical diffusion [12]. For large q (i.e., small length scales) this Brownian scaling breaks down to a stretched exponential with $\beta < 1$, which can attributed to the presence of dynamic heterogeneities due to caging.

Returning to the case of fixed $qD = 2.14$, we plot τ as a function of ϕ in Fig. 5. A significant slowing down of the dynamics can be seen at high ϕ as crystallization is approached. It is highly surprising that this slowing down with ϕ is well described by the Vogel-Fulcher law [19] as found in many glass forming systems,

$$\tau \sim \exp[A/(\phi_c - \phi)], \tag{3}$$

where $A = 0.094 \pm 0.004$ is a fitting parameter but $\phi_c = 0.719 \pm 0.007$ is the filling fraction for crystallization which was determined independently from experiments [14]. A power-law fit was not as satisfactory. Note that, as the fluid goes through the transition from isotropic fluid to the intermediate phase (at $\phi_l = 0.652$), τ shows no particular feature. This functional dependence of the re-

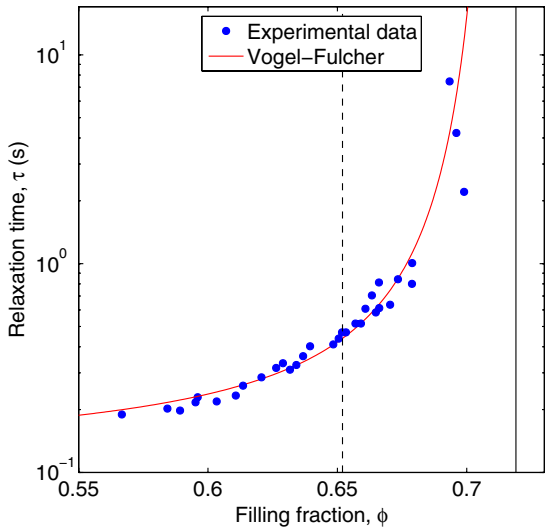

FIG. 5 (color online). Relaxation time, τ, extracted from the intermediate scattering function as a function of filling fraction. The solid line is a fit to the Vogel-Fulcher law of Eq. (3). Dashed and solid lines represent the location of the liquidus and solidus points, respectively.

laxation has also recently been found within the granular context by Fierro *et al.* [20] in a numerical lattice model.

In summary, we have studied the dynamics of a uniformly heated granular fluid. We have observed a number of features typically associated with dense liquid behavior in molecular and colloidal systems, namely: prominence of cages, development of a plateau in the MSD and ISF with the breakdown of the Brownian diffusive behavior, and a Vogel-Fulcher relaxation. Even though the emergence of the plateaus and the relaxation time grow smoothly past the liquidus point, they become particularly visible for $\phi \geq \phi_l$. In particular, our results can be directly compared to both experiments [6] and simulations [10] of quasi-2D colloidal particles. This is surprising since our experiment is fundamentally different: it is intrinsically far from equilibrium since energy is not conserved, the constituent particles are macroscopic, and it is known that for monodisperse and quasi-2D systems such as ours there is no ideal glass transition [21] (the phase diagram is fluid, intermediate phase, and crystal). In the absence of an amorphous structural glass, we propose that the spatially uniform stochastic way of injecting energy along with a process of structural arrest provided by crystallization [14] are at play to account for the many observed similarities. This suggests that theoretical frameworks previously developed for dense thermal liquids, for example, MCT [7], might shed some light to the description of excited granular materials.

This material is based upon work supported by the National Science Foundation under Grant No. 0134837. P. M. R. was partially funded by the Portuguese Ministry of Science (POCTI) and the European Union (MECHPLANT NEST-Adventure).

*Current address: Laboratoire PMMH (UMR7636 CNRS-ESPCI-P6-P7), 10 rue Vauquelin, 75231 Paris, France. Email address: preis@pmmh.espci.fr
†Email address: shattuck@ccny.cuny.edu

[1] H. Jaeger and S. Nagel, Science **255**, 1523 (1992); H. Jaeger, S. Nagel, and R. Behringer Rev. Mod. Phys. **68**, 1259 (1996).
[2] I. Goldhirsch, Annu. Rev. Fluid Mech. **35**, 267 (2003).
[3] A. J. Liu and S. R. Nagel, Nature (London) **396**, 21 (1998).
[4] P. N. Pusey and W. van Megen, Physica (Amsterdam) **157A**, 705 (1989); W. van Megen and S. M. Underwood, Phys. Rev. E **47**, 248 (1993).
[5] E. R. Weeks, J. C. Crocker, A. C. Levitt, A. Schofield, and D. A. Weitz, Science **287**, 627 (2000).
[6] H. König, R. Hund, Z. Zahn, and G. Maret Eur. Phys. J. E **18**, 287 (2005).
[7] W. Götze, in *Liquids, Freezing and Glass Transition*, Proceedings of the Les Houches Summer School, Session LI, edited by J. P. Hansen, D. Levesque, and J. Zinn-Justin (North-Holland, Amsterdam, 1991).
[8] L. F. Cugliandolo, in *Slow Relaxations and Nonequilibrium Dynamics in Condensed Matter*, Proceedings of the Les Houches Summer School, Session LXXVII, edited by J.-L. Barrat, J. Dalibard, J. Kurchan, and M. V. Feigelman (Springer, New York, 2004), p. 367.
[9] J.-L. Barrat, J.-N. Roux, and J.-P. Hansen, Chem. Phys. **149**, 197 (1990).
[10] M. M. Hurley and P. Harrowell, Phys. Rev. E **52**, 1694 (1995); R. Zangi and S. A. Rice Phys. Rev. Lett. **92**, 035502 (2004).
[11] O. Pouliquen, M. Belzons, and M. Nicolas, Phys. Rev. Lett. **91**, 014301 (2003).
[12] G. Marty and O. Dauchot, Phys. Rev. Lett. **94**, 015701 (2005); O. Dauchot, G. Marty, and G. Biroli, Phys. Rev. Lett. **95**, 265701 (2005).
[13] A. R. Abate and D. J. Durian, Phys. Rev. E **74**, 031308 (2006).
[14] P. M. Reis, R. A. Ingale, and M. D. Shattuck, Phys. Rev. Lett. **96**, 258001 (2006).
[15] A. Jaster, Phys. Lett. A **330**, 120 (2004).
[16] H. Sillescu, J. Non-Cryst. Solids **243**, 81 (1999); M. D. Ediger, Annu. Rev. Phys. Chem. **51**, 99 (2000).
[17] P. M. Reis, R. A. Ingale, and M. D. Shattuck, cond-mat/0611024 [Phys. Rev. E (to be published)].
[18] J. S. Olafsen and J. S. Urbach, Phys. Rev. Lett. **81**, 4369 (1998).
[19] H. Vogel Z. Phys. **22**, 645 (1921); G. S. Fulcher J. Am. Ceram. Soc. **8**, 339 (1925).
[20] A. Fierro, M. Nicodemi, M. Tarzia, A. de Candia, and A. Coniglio, Phys. Rev. E **71**, 061305 (2005).
[21] L. Santen and W. Krauth, Nature (London) **405**, 550 (2000); A. Donev, F. H. Stillinger, and S. Torquato, Phys. Rev. Lett. **96**, 225502 (2006).